Glutaric acid affects pericyte contractility and migration: possible implications for GA-I pathogenesis

Eugenia Isasi[1,2], Nils Korte[4], Verónica Abudara[3], David Attwell[4] & Silvia Olivera-Bravo[1*]

[1]Neurobiología Celular y Molecular, Instituto Clemente Estable (IIBCE), Montevideo, UY.
[2]Departmento de Histología y Embriología, Facultad de Medicina, Universidad de la República, Montevideo, UY.
[3]Departmento de Fisiología, Facultad de Medicina, Universidad de la República, Montevideo, UY.
[4]Department of Neuroscience, Physiology & Pharmacology, University College London (UCL), London, UK.

*** Corresponding author:**
Mailing address: 3318, Italia Av., 11600 Montevideo, URUGUAY
Tel number: +5982 4871616
Fax number: +5982 4875461
E-mail: solivera2011@gmail.com

Abstract
Glutaric Acidemia I (GA-I) is an inherited neurometabolic childhood disease characterized by bilateral striatal neurodegeneration upon brain accumulation of millimolar concentrations of glutaric acid (GA) and related metabolites. Vascular dysfunction, including abnormal cerebral blood flow and blood-brain barrier damage, is an early pathological feature in GA-I, although the affected cellular targets and underlying mechanisms remain unknown. In the present study, we have assessed the effects of GA on capillary pericyte contractility in cerebral cortical slices and pericyte cultures, as well as on the survival, proliferation and migration of cultured pericytes. GA induced a significant reduction in capillary diameter at distances up to ~10 μm from the center of pericyte somata. However, GA did not affect the contractility of cultured pericytes, suggesting that the response elicited in slices may involve GA evoking pericyte contraction by acting on other cellular components of the neurovascular unit. Moreover, GA indirectly inhibited migration of cultured pericytes, an effect that was dependent on soluble glial factors since it was observed upon application of conditioned media from GA-treated astrocytes (CM-GA), but not upon direct GA addition to the medium. Remarkably, CM-GA showed increased expression of cytokines and growth factors that might mediate the effects of increased GA levels not only on pericyte migration but also on vascular permeability and angiogenesis. These data suggest that some effects elicited by GA might be produced by altering astrocyte-pericyte communication, rather than directly acting on pericytes. Importantly, GA-evoked alteration of capillary pericyte contractility may account for the reduced cerebral blood flow observed in GA-I patients.
Keywords: Glutaric acidemia type 1, glutaric acid, astrocytes, pericyte, cell migration, capillary contractility, astrocyte-conditioned media

Abbreviations: Blood brain barrier (BBB), glutaric academia type I (GA-I), glutaric acid (GA), 3-hydroxyglutaric acid (3-OHGA), glutaryl-CoA dehydrogenase (GCDH), receptor β of the platelet derived growth factor (PDGFRβ), neural/glial antigen 2 (NG2), alpha smooth muscle actin (αSMA), astrocyte conditioned media (CM), GA-treated astrocyte conditioned media (CM-GA), control astrocyte conditioned media (CM-C), artificial cerebrospinal fluid (aCSF), propidium iodide (PI).

Introduction

Glutaric acidemia type I (GA-I) is a rare autosomal recessive metabolic disorder caused by deficiency of the mitochondrial enzyme glutaryl-CoA dehydrogenase (GCDH), which is involved in the catabolism of lysine, hydroxyl-lysine and tryptophan. Loss of functional GCDH leads to the accumulation of up to millimolar levels of glutaric acid (GA) and related metabolites in body fluids and tissues [1-3]. GA-I is primarily a neurological disorder, the pathological hallmarks of which include striatal degeneration (expressed as delayed motor responses or regression during infancy), gliosis, diffuse and progressive white-matter abnormalities, and early vascular dysfunction [1,3,4].

The most prominent vascular defects in GA-I include blood-brain barrier (BBB) breakdown, subdural effusions, chronic extravasation from trans-arachnoid vessels and intradural and retinal hemorrhages that usually occur before the triggering of striatal damage [1-3, 5-8]. Significant expansion of the cerebrospinal fluid volume and cerebral blood volume, as well as an elevation of the mean capillary transit time, was also found in some children [6,9]. Blood-brain barrier breakdown together with vasogenic oedema, distention of striatal capillaries, enlarged vessels and hemorrhagic areas were also found in Gcdh -/- mice, once exposed to a high lysine diet that elevated GA levels [10].

The few molecular studies focused on GA-I vascular dysfunction show that cerebral cortices of Gcdh-/- mice have higher mRNA expression of vascular endothelial growth factors A and C, and of angiogenin, all of which are involved in regulating angiogenesis and vascular permeability [11]. In addition, endothelial cells were damaged by incubation with 3-hydroxyl-glutaric acid (at concentrations larger than those found in patients during crises [2]) as well as in Gcdh-/- mice fed a high lysine diet [10], suggesting this may disturb the integrity of vascular structures [12].

Recently, we have reported that a single intracerebral dose of GA given to rat pups affects key components of the neurovascular unit (NVU), evoking decreased expression of aquaporin 4 in astrocyte end-feet, loss of PDGFRβ positive pericytes surrounding micro-vessels, and decreased laminin associated with blood vessels, all leading to significant BBB leakage [13]. These findings, in the context of previous reports showing that GA induced astrocyte increased proliferation, oxidative stress and decreased support to neurons [14,15], led us to propose that effects of GA-I evoked metabolites on pericytes, acting either directly or via astrocytes, may have a role in the vascular dysfunction reported in the disease.

Moreover, as Strauss et al. [6,16] hypothesized that vascular defects may depend on hemodynamic alterations caused by glutarate accumulation in the brain, in the present study we evaluated whether a pathophysiological concentration of GA affected brain capillary contractility in slices and in isolated brain pericyte cultures. In addition, we assessed the effects of GA and GA-elicited astrocytic soluble factors on the proliferation and migration of cultured pericytes. Finally, we evaluated the cytokine composition of astrocyte-derived soluble factors released from GA-treated cells.

Materials and Methods

Ethical statement

This study was performed in accordance with the Principles of Laboratory Animal Care, National Institute of Health of United States of America, NIH, publication no. 85-23 (2011 revision), and approved by the IIBCE Ethical Committee for the Care and Use of Laboratory Animals and from the National Committee for Laboratory Animal Care (CNEA) from Uruguay. All efforts were made to minimize suffering, discomfort and stress to the animals. The number of animals employed in this work was the necessary to produce reliable scientific data.

Chemicals

Dulbecco's modified Eagle's medium (DMEM), fetal bovine serum (FBS), 100 IU penicillin/100 mg/ml streptomycin and trypsin were purchased from Invitrogen (Carlsbad, CA, USA). Collagenase type I, DNAase I, poly-D-lysine, GA and all other chemicals of analytical grade were obtained from Sigma-Aldrich (USA). Rat Cytokine Antibody Array C2 was purchased from RayBiotech (Norcross, GA, USA).

Animals

Primary cell cultures and acute brain slices were obtained from *Sprague-Dawley* (SD) rats bred at IIBCE and UCL. Animals were housed in cages with food and water *ad libitum*, controlled temperature and 12 hr light/dark cycles. Institutional guidelines based on National and International laws for protection of vertebrate animals used for scientific purposes were followed. All procedures were carried out in accordance with the guidelines of the IIBCE Ethical Committee and the UK Animals (Scientific Procedures) Act 1986 and subsequent legislation. For cell culture experiments, 7 separate astrocyte cultures were obtained from the cerebral cortices of 7 rat pups of postnatal day 1 (P1) and 7 pericyte cultures were obtained from 7 whole brains of 2-3 week old rats. For experiments on acute brain slices of P21 SD rats, tissue was obtained from at least 4 animals on at least 4 different experimental days.

Brain slice preparation

As previously described [17,18], 240-300 µm thick coronal cortical slices were prepared from P21 rats on a vibratome in ice-cold oxygenated (95% O_2, 5% CO_2) solution containing (in mM) 93 N-methyl-D-glucamine chloride, 2.5 KCl, 30 $NaHCO_3$, 10 $MgCl_2$, 1.2 NaH_2PO_4, 25 glucose, 0.5 $CaCl_2$, 20 HEPES, 5 sodium ascorbate, 3 sodium pyruvate and 1 kynurenic acid. The slices were incubated at 34°C in the same solution for 15–20 min, then transferred to a similar solution but containing (in mM) 93 NaCl, 1 $MgCl_2$ and 2 $CaCl_2$, and then incubated at room temperature (21–23 °C) until used in experiments.

Imaging of capillaries in brain slices

Slices (300 µm thick) were perfused with artificial cerebrospinal fluid (aCSF) containing (in mM) 124 NaCl, 2.5 KCl, 26 $NaHCO_3$, 1 $MgCl_2$, 2 $CaCl_2$, 1 NaH_2PO_4, 10 glucose, 1 sodium ascorbate, heated to 31–35 °C and gassed with 20% O_2, 5% CO_2 and 75% N_2 to produce a physiological [O_2] around the imaged cells [19]. Capillaries were imaged using differential interference contrast (DIC) microscopy at 20–50 µm depth within layers III–VI of cortical slices containing the motor and prefrontal cortices, employing a 40x water immersion objective, a Coolsnap HQ2 CCD camera, and ImagePro Plus acquisition software. Images were acquired every 30 s, with an exposure time of 100 ms and a pixel size of 160 nm. Vessel internal diameters were measured by manually placing a measurement line perpendicular to the vessel cross section at locations close (<10 µm) or far (20-25 µm distance) from the center of pericyte soma. Measurements were made using Metamorph software or Image J (NIH, USA). To assess GA effects on capillary diameter, images were obtained in basal condition (5 min perfusion with acSF) and after the addition of 1 mM GA (pH=7.4) for 20 min or endothelin 1 (10 nM, which was used as a positive control to assess whether pericytes were responsive to contractile agonists).

Capillary diameters were also measured in fixed brain slices (240 µm thick) that were previously incubated with aCSF or aCSF containing 1 mM GA (pH=7.4) for 1 hr at 37ºC. After fixation, slices were stained with fluorescent isolectin B_4 (10 µg/ml) and Hoestch 33342 (1 µg/ml) and visualized with a confocal microscope Zeiss LSM700. Z-stacks of 23 µm width (excluding the first 30 µm from the surface) from different cortical regions were acquired. Vessel diameters in IB_4 images were measured at different distances (up to 10 µm) from the center of pericyte somata by using Image J (NIH, USA).

Assessing pericyte death in slices

This procedure was carried out as previously described in Hall et al. ([19]). Brain slices of 240 µm thickness were incubated in a multi-well plate, with oxygen blown gently at the surface in aCSF alone or aCSF containing 1 mM or 5 mM GA (pH=7.4). All extracellular solutions contained isolectin B_4 (10 µg/ml) to label the basement membranes (and pericytes wrapped in it) and 7.5 µM propidium iodide (PI) to label cells with membranes that had become non-specifically permeable [19]. After 2 hr of incubation, slices were fixed in 4% paraformaldehyde (PFA, pH=7.4), and imaged on a Zeiss LSM700 confocal microscope. To avoid counting cells killed by the slicing procedure, quantification of the percentage of pericytes that were dead excluded cells within 12 µm of the slice surface.

Astrocyte primary cultures to obtain conditioned media

Astrocyte primary cultures were prepared from SD rats aged 1–2 days as described by Cassina et al. [20] with minor modifications. Briefly, glial mixed cultures were obtained from cortices that were dissociated with trypsin and by mechanical pipetting, seeded in proliferation media containing DMEM supplemented with 10% FBS, 3.6 g/l HEPES, 1.2 g/l $NaHCO_3$ plus penicillin/streptomycin. Once 100% confluent, cultures were depleted of other contaminant glial cells by continuous shaking for 48 h. Cultures containing at least 98% glial fibrillary acid protein (GFAP)-positive astrocytes and a lack of OX42-positive microglial cells were left resting for a week. Then, cells were trypsinised, harvested on 60 mm Petri dishes or 25 cm^2 T flasks at a density of 1.5-2.0 x $10^4/cm^2$ and maintained in proliferation media. Once confluent, cultures enriched in astrocytes were exposed to 5 mM GA (pH=7.4) or vehicle for 24 hr. The medium was then removed, cells were thoroughly washed with 10 mM phosphate buffered saline solution (PBS, pH=7.4) and incubated in proliferation media. After 24 hr, the conditioned media from control (CM-C) and GA-treated astrocytes (CM-GA) were collected by centrifugation and immediately applied to pericyte cultures.

Pericyte primary cultures

Pericyte cultures were prepared as described by Tigges et al. [21] with some modifications. Briefly, 2-3 week old rats were euthanized and brains quickly extracted and placed in PBS. The olfactory bulbs, cerebellum and medulla were dissected away and meninges were carefully removed. The rest of the brain was minced thoroughly with a sterilized razor blade and incubated in DMEM containing 0.225 mg/ml collagenase I, 5 mM $CaCl_2$ and 40 µg/ml DNase I. After 1 hr incubation at 37°C, the digested brain tissue was homogenized manually and then filtered through an 80 µm mesh. The homogenized cells were mixed with 1.7 volumes of 22% bovine serum albumin (BSA) solution and centrifuged at 2000 rpm for 10 min. The pellet was re-suspended in DMEM supplemented with 10% FBS and isolated brain

microvessel fragments were seeded on 35 mm Petri dishes pre-coated with 5 µg/cm^2 collagen I. Once grown to confluence (7-8 days later), cells were detached with 0.05% trypsin (5 min), centrifuged (1000 rpm, 10 min) and plated on uncovered petri dishes at a 1:3 dilution in supplemented DMEM. This step was repeated (second passage) and cells were maintained until confluent (~ 1 week). At this stage, cultures consisted of at least 95% neural/glial antigen 2 (NG2) and PDGFRβ expressing pericytes, ~1% of von Willebrand factor expressing endothelial cells and less than 4% of GFAP expressing astrocytes.

Pericyte migration and proliferation assays

To test whether GA can affect pericyte migration, confluent second-passage pericyte cultures were scratched manually with a sterile 0.1-10 µL pipette tip. Detached cells were removed with 3 rinses of PBS and then cultures were exposed to 5 mM GA (pH=7.4) or PBS (control). In other experiments, scratched cells were treated with CM-C or CM-GA (1:1 dilution) to analyze the effect of astrocyte-conditioned media on pericyte migration. Images were taken at 0, 24 and 48 hr after the scratch, and cell-free areas measured at each time and condition. To test the effects of GA or astrocyte-conditioned media on the proliferation of scratched pericytes, in some experiments 40 µM bromodeoxyuridine (BrdU) was added to the culture media with each treatment.

Contractility assessment

Confluent second-passage pericyte cultures were incubated with 5 mM GA (pH=7.4), CM-C, CM-GA or 100 µM ATP (positive control) [22,23] for 2 hr (at 37ºC, with 5% CO_2/95% O_2). After that, pericytes were washed with PBS, fixed with 4% PFA (20 min, RT) and visualized using white light and fluorescence in an inverted microscope Olympus IX-81. Pericyte contraction was clearly seen as a change in cell morphology [22] that included retraction of the cell body, emergence of visible processes and smaller nuclei. The percentage of contracted cells (normalized by the total number of Hoechst 33342-stained nuclei), was evaluated.

Cell viability assay

The sulforhodamine B (SRB) assay is based on the measurement of cellular protein content. The assay was performed according to manufacturer's instructions (Sigma-Aldrich). Briefly, 10,000-20,000 pericytes were seeded in each well of a 96-well plate. Pericytes were grown to confluence and incubated with 5 mM GA, CM-C or CM-GA during 24 hr. After that, cell monolayers were fixed with 10% (wt/vol) trichloroacetic acid (1 hr, 4ºC), left to dry and stained with SRB (0,4%, 30 min), after which the excess dye was removed by washing repeatedly with 1% (vol/vol) acetic acid. The protein-bound dye was dissolved in 10 mM Tris base solution for determination of optical density at 565 nm and background multiwell absorbance at 690 nm, by using a Varioskan microplate reader.

Immunocytochemistry

Pericytes were recognized by immunolabeling against 3 prototypic markers: alpha smooth muscle actin (αSMA), PDGFRβ and NG2 [24]. To perform the immunolabeling, cells were washed with PBS, fixed with 4% PFA, permeabilized with 0.1% Triton X-100, blocked with 5% BSA and incubated overnight at 4°C with one or two of the following antibodies: anti-αSMA (1:100, SIGMA), anti-PDGFRβ (1:100, abcam), anti-NG2 (1:250, Millipore). Cells were quickly washed and incubated for 90 min at RT in 1:500 dilutions of secondary antibodies conjugated to Alexa Fluor 488 or 546. For visualization of the actin cytoskeleton, fixed and permeabilized cells were incubated with phalloidin conjugated to TRITC (1:250, Invitrogen) for 20 min at RT and rinsed with PBS afterwards. All cells were mounted with 1:1 glycerol-PBS containing 1 µg/ml Hoechst 33342 and were visualized with a confocal microscope Olympus FV300 and Zeiss LSM800.

Cell proliferation was assessed by immunocytochemical detection of BrdU at 48 hr after the scratch. To do this, pericyte cultures were fixed with 4% PFA (20 min, RT), washed with PBS and underwent DNA denaturation with 2 N HCl for 45 min at RT. After several washes with PBS, cultures were incubated in blocking buffer containing 5% BSA for 1 hr, followed by incubation with an anti-BrdU antibody (1:500, Dako) overnight at 4°C. After three washes with PBS, cultures were incubated with a secondary antibody conjugated to Alexa Fluor 488 (1/500, Invitrogen). BrdU-positive cells were counted and proliferation rate was expressed as the percentage of cells labeled with Hoechst 33342.

Ethidium bromide staining

Ethidium bromide (EtBr) is a cationic probe, which is normally cell membrane impermeant, but when applied in the extracellular milieu the dye can enter into certain types of cell through diverse mechanisms including large pore channels and pumps [25,26]. Once intracellular, EtBr fluoresces when it intercalates into nucleic acid strands. Pericyte cultures were incubated with 10 nM EtBr at 5% CO_2 and 37ºC for 20 min, then washed several times in PBS and finally fixed with 4% PFA (30 min, RT). After mounting with glycerol-PBS containing Hoechst 33342 (1 µg/ml), cells were imaged using an Olympus FV300 and Zeiss LSM800 confocal microscope with an excitation laser of 488 nm and a bandpass emission filter of 630-660 nm.

Live cell imaging

Pericyte cultures were seeded on a Lab-Tek® 4-well chamber slide in a range of 20-25,000 cells/well and maintained confluent in DMEM supplemented with 10% FBS. Cultures were maintained at 37ºC and 5% CO_2 and incubated with 5 mM GA (pH=7.4), 100 nM ATP or PBS (control). Images were acquired every 1 min for 35-40 min using a Leica CTR6500 TCS5P6 confocal microscope with a motorized stage. Quantification of cell-free area was performed by using ImageJ software (NIH, USA).

Rat cytokine array

Astrocytes grown to confluence in 75 cm^2 T-flasks were treated with GA (5 mM, 24 hr) or PBS, followed by incubation in DMEM without FBS for 24 hr. Conditioned medium was collected and centrifuged (10 min, 2000 rpm), and the supernatant was frozen at -20ºC. After that, conditioned medium was concentrated by using a Millipore Centricon® with an ultracel YM-3 membrane, 3000 nominal molecular weight limit, according to manufacturer instructions. Quantitation of total protein content was determined by using a bicinchoninic acid assay or Bradford assay. The expression level of 32 soluble cytokines present in astrocyte conditioned media was assessed with the Rat Cytokine Antibody Array C2 kit from RayBiotech according to the manufacturer's instructions. Images were taken with a CCD camera for chemiluminescence detection. The total integrated density of the same area in each spot was measured with Image J software (NIH, USA), values of negative controls and background were subtracted, and then normalized to the mean value of the 6 positive controls present in each membrane. To compare signals in different membranes, values were corrected by the ratio among the control positive values of the comparing membranes. Finally, the comparison between the values of each cytokine was made as the fold among signals in CM-GA vs CM-C. Two independent cytokine array experiments were conducted.

Calculation of effect of vessel constriction on flow

We assume that pericytes are regularly spaced on capillaries at an interval of 2L. For flow governed by Poiseuille's law, the resistance of a segment of capillary of length L (from a pericyte soma to midway between two pericytes) and radius r_1 is given by

$$k.L/r_1^4$$

where k is a constant. If GA-induced pericyte contraction reduces the capillary diameter from a value of r_1 at the midpoint between pericytes to r_2 near the pericyte soma, then if this reduction is linear with distance the resistance of the capillary segment from the soma to the midpoint is given by

$$k.L.(r_1^2 + r_1.r_2 + r_2^2)/(3.r_1^3.r_2^3)$$

so the factor by which the resistance is altered is

$$[1 + (r_1/r_2) + (r_1/r_2)^2].(r_1/r_2)/3$$

This was used to calculate the predicted flow reduction to be produced by pericyte constriction in Fig. 1 and the main text.

Statistical analysis

Data analysis was performed with Graphpad Prism 3.0 and 6.0 by using a Student's *t*-test for parametric data or a Mann-Whitney test for non-parametric data to compare two groups. P-values were corrected for multiple comparisons using a one-way ANOVA followed by Tukey or Bonferroni post-hoc tests for parametric data or a Kruskal Wallis test followed by Dunn's test for non-parametric data. A p-value <0.05 was considered statistically significant. Values were represented by using the mean±SEM or the median and interquartile range as appropriate.

Results

GA produced capillary constriction in cerebral cortical slices

Coronal slices from P21 rats were perfused with aCSF (5 min) or aCSF containing 1 mM GA (20 min) while imaging the capillaries. GA evoked a capillary constriction of ~16% near pericyte somata (p=0.04, n=10) after 25 min of incubation. Vessel diameters near pericyte somata were measured at <10 µm from the center of pericyte somata as stated in the Methods (Figure 1 a, b). Control experiments were done with aCSF alone (n=3) and as a positive control slices were incubated with 10 nM endothelin 1 (n=4), which evoked a 40% capillary diameter reduction at 15.5 min (p=0.008). To estimate the effects of GA induced-capillary constriction on cerebral blood flow, Poiseuille's law was applied as described in the Methods. The observed reduction of 16% in vessel diameter near pericyte somata is predicted to increase the capillary resistance by a factor of 1.43.

Other sets of slices were perfused with aCSF alone (controls) or aCSF containing 1mM GA for 1 hr and submitted to PFA fixation and IB_4 staining. Then, confocal stack images were taken and vessel diameters were measured at <10 µm from the center of pericyte somata. There was a 23% reduction in capillary diameters of slices exposed to GA compared with controls (p=0.0006) (Figure 1 c, d).

Vessel constriction was not related to pericyte death in rigor as reported in ischemia (see [19]). Pericyte death assessment by propidium iodide incorporation did not show any significant difference between GA-treated slices and controls (Figure S1 a, b).

GA did not affect pericyte contraction in culture

To assess whether the GA-induced constriction of capillaries is due to a direct effect of GA on pericytes, we tested whether GA evokes the contraction of isolated pericytes obtained from brain microvessels, as described by Tigges et al. [21] with minor modifications. Second passage pericyte cultures expressed the three prototypical pericyte markers NG2, PDGFRβ and αSMA, but not the endothelial cell marker von Willebrand Factor (vWF) or the astrocyte marker GFAP (Figure 2 a, b). Pericyte cultures also responded typically to the vasoactive agents ATP (10 μM) or adenosine (10 μM), by changing cell morphology in accordance with ATP constricting them and maintaining their flat morphology upon adenosine exposure (Figure 2 c). However, when pericyte cultures were incubated with 5 mM GA, 100 μM ATP (a positive control) or vehicle (negative control) for 2 hr, only ATP, but not GA, caused visible morphological changes, that appear as a reduction of soma and nuclei size together with the emergence of conspicuous cellular processes (Figure 3 a, c). These morphological changes were also accompanied by a re-arrangement of actin filaments stained with phalloidin (Figure 3 b). In addition, live cell imaging of pericytes exposed to 5 mM GA, 100 μM ATP or vehicle for 35 min, confirmed that progressive morphological changes occur only in the ATP condition, and not with GA, as shown by an increased cell-free area between contracted pericytes (Figure 3 d, e). These results show that GA does not have a direct effect on pericyte contractility in pericyte enriched cultures.

To test whether GA is toxic to pericytes, they were challenged with 1 and 5 mM GA or PBS for 24 hr. Cell viability was assessed with an SRB assay. This showed that, at the concentrations used, GA did not affect pericyte viability (Figure S1 d). Furthermore, no changes in morphology, in actin filament arrangement or in PDGFRβ expression were found after 24 hr exposure of cultured pericytes to 5mM GA (Figure S1 c, e). All together, these data show that GA does not constrict isolated cultured pericytes. Although it is possible that pericytes change the proteins they express in culture, these data suggest the GA-evoked capillary constriction seen in brain slices may be an indirect effect mediated by GA acting on cells in the slice other than pericytes.

Because GA was previously reported to induce astrocyte dysfunction [14,27], we tested whether factors released by astrocytes in response to GA regulate pericyte contractility in cultures. Cultured pericytes incubated with conditioned medium (CM) from astrocytes treated with GA (CM-GA) or vehicle (CM-C) showed a remarkable change in pericyte morphology after 2 hr, which resembled that observed with ATP treatment (Figure 4 a). Interestingly, the increase in number of contracted pericytes was similar in CM-C and CM-GA conditions (Figure 4 b). This suggests that astrocytic soluble factors affect pericyte contractility in culture independently of the presence of GA, and suggests that GA might not generate pericyte contraction by evoking the release of substances from astrocytes.

Astrocyte CM-GA delayed pericyte migration

Cultured pericytes were submitted to a scratch wound assay and then incubated with vehicle (controls), 5 mM GA, CM-C or CM-GA for 48 hr, and cell-free area was quantified over time. As expected, a progressive reduction of cell-free area was observed in all experimental conditions because cells at the wound edge proliferate and migrate [28]. However, CM-GA exposure caused a delay in the closure of the scratch (compared to CM-C), as shown by a significantly larger cell-free area at 24 and 48 hr, respectively (Figure 5 a, b). On the other hand, cell-free areas in scratched cells directly treated with GA did not show any significant differences with respect to controls. Moreover, the delay in the scratch closure caused by CM-GA incubation cannot be attributed to reduced cell proliferation, since the number of BrdU+/Hoechst+ cells in the scratch region was similar to that found in control cultures (Figure 5 d). Thus, CM-GA did not affect pericyte proliferation, but delayed pericyte migration as a result of soluble factors secreted by astrocytes upon GA treatment.

Differential expression of cytokines in CM-GA

To further understand which astrocytic soluble factors could be affecting pericyte migration in cultures, we analyzed CM-C and CM-GA using commercial rat cytokine arrays. Interestingly, the levels of several cytokines seem to be increased in CM-GA compared with CM-C (Figure 6). We observed higher expression of the tissue inhibitor of metalloproteinase 1 (TIMP-1), which inhibits the matrix metalloproteinases (MMPs) that promote pericyte migration by degrading several components of the extracellular matrix [29], vascular endothelial growth factor-A (VEGF-A), intracellular cell adhesion molecule-1 (ICAM-1), cytokine-induced neutrophil chemoattractant-1 (CINC-1), LIX, monocyte chemo-attractant protein-1 (MCP-1), macrophage inflammatory protein-3 (MIP3) and L-selectin, all of which have important effects on vascular permeability and inflammation [30].

Discussion

Since cerebrovascular changes contribute to neuropathology in GA-I, and the majority of the resistance to blood flow within the brain parenchyma is located in capillaries [31], in the present work we have evaluated the effects of GA on capillary constriction in acute cortical slices and in primary cultured

pericytes.

Experiments on pericytes in situ in brain slices showed that applying GA at concentrations found in GA-I patients, or in the Gcdh-/- mouse model of GA-I [2,10,32], reduced cortical capillary diameters by ~16%, which according to Poiseuille's law may cause an increase of capillary resistance of 43% and a reduction of 30% in blood flow. The data obtained are in accordance with those of Strauss et al. [7] who analyzed Amish GA-I patients ranging from lack of evident striatal injuries to others presenting dystonia and striatal lesions in different disease conditions and ages. In that study, perfusion scans from six patients showed that tissue blood flow did not undergo a normal developmental surge, as usually occurs over the first few years of life, and that four patients had a significant reduction of cerebral blood flow sometimes accompanied by increased cerebral blood volume and mean transit time. Haemodynamic alterations caused by brain glutarate accumulation may therefore contribute to striatal necrosis in GA-I [6,7]. Because a subset of contractile pericytes adjusts capillary diameter and the majority of the vascular resistance in the CNS is located in capillaries [19,24,31,33-35], it is likely that GA impairs microvascular perfusion by acting on pericytes, as found in this work.

GA, however, did not elicit the contraction of isolated cultured pericytes, making the possibility of a direct effect unlikely, and suggesting that GA-induced pericyte contractility in slices may be the result of signaling between cells of the NVU. As we previously demonstrated that GA induced astrocytic dysfunction *in vivo* and in cultures by enhancing cell proliferation, mitochondrial dysfunction, oxidative stress and neurotoxicity [14,27,35], we tested whether astrocyte soluble factors released by GA might elicit contraction of cultured pericytes. Although conditioned medium obtained from both control (CM-C) and GA-treated (CM-GA) astrocytes caused morphological changes in cultured pericytes that resembled those evoked by the vasoconstrictor ATP, CM-GA did not increase pericyte contractility when compared to CM-C. Soluble factors released by astrocytes may therefore elicit a contractile response in pericytes, however, either the release of these factors is independent of GA or the release of these factors even in control conditions is sufficient to evoke a saturating contraction. Nevertheless, the signaling mechanism by which GA induces pericyte contaction is likely of a multicellular nature and requires further study.

In contrast, exposure to CM-GA, but not to CM-C, GA itself or vehicle, inhibited pericyte migration without changing proliferation in a scratch wound assay. Pericyte migration evoked by endothelial PDGF-β - pericyte PDGFRβ signaling is an important process during brain angiogenesis and is essential for the normal structure and function of the brain vasculature [36-38]. Defects in pericyte migration during early and post-natal development in GA-I patients could therefore disrupt pericyte coverage of vessels and induce vascular dysfunction. In this regard, increased GA levels could affect brain structure, not only during early infancy, but also prenatally [39]. The link between blood flow alterations in GA-I patients and pericyte dysfunction or loss requires further study.

We identified several soluble factors released from astrocytes that may inhibit pericyte migration. Among the cytokines that were elevated in concentration in CM-GA relative to CM-C, are TIMP-1, ICAM-1 and VEGF-A, which are important in regulating vascular morphogenesis/regression [40], angiogenesis [41] and BBB permeability [42,43]. Therefore, GA-induced astrocytic dysfunction could alter not only pericyte migration, but also the physiology of other neurovascular unit cells, through the release of soluble factors.

In summary, we demonstrate that acutely applied GA increases pericyte contractility and decreases pericyte migration. These effects are expected to decrease cerebral blood flow and alter vasculogenesis. Together with the previously-demonstrated effect of GA to disrupt the BBB [13], these actions are likely to contribute to clinically important vascular abnormalities in GA-I.

References

[1] Hoffmann GF, Athanassopoulos S, Burlina AB, Duran M, de Klerk JB, Lehnert W, Leonard JV, Monavari AA, Muller E, Muntau AC, Naughten ER, Plecko-Starting B, Superti-Furga A, Zschocke J, Christensen E (1996) Clinical course, early diagnosis, treatment, and prevention of disease in glutaryl-CoA dehydrogenase deficiency. Neuropediatrics 27:115–123. https://doi.org/10.1055/s-2007-973761

[2] Funk CB, Prasad AN, Frosk P, Sauer S, Kolker S, Greenberg CR, Del Bigio MR (2005) Neuropathological, biochemical and molecular findings in a glutaric acidemia type 1 cohort. Brain 128:711–722. https://doi.org/10.1093/brain/awh401

[3] Boy N, Mühlhausen C, Maier EM, Heringer J, Assmann B, et al (2017) Proposed recommendations for diagnosing and managing individuals with glutaric aciduria type I: second revision. J Inherit Metab Dis. 40(1):75-101. https://doi.org/10.1007/s10545-016-9999-9

[4] Goodman SI, Markey SP, Moe PG, Miles BS, Teng CC (1975) Glutaric aciduria; a "new" disorder of amino acid metabolism. Biochem Med. 12(1):12-21. https://doi.org/10.1016/0006-2944 (75)90091-5

[5] Knapp JF, Soden SE, Dasouki MJ, Walsh IR (2002) A 9-month-old baby with subdural hematomas, retinal hemorrhages, and developmental delay. Pediatr Emerg Care 18(1):44-47. https://doi.org/10.1097/00006565-200202000-00014

[6] Strauss KA, Lazovic J, Wintermark M, Morton DH (2007) Multimodal imaging of striatal degeneration in Amish patients with glutaryl-CoA dehydrogenase deficiency. Brain 130:1905-1920. https://doi.org/10.1093/brain/awm058

[7] Strauss KA, Donnelly P, Wintermark M (2010) Cerebral haemodynamics in patients with glutaryl-coenzyme A dehydrogenase deficiency. Brain 133:76-92. https://doi.org/10.1093/brain/awp297

[8] Harting I, Neumaier-Probst E, Seitz A, Maier EM, Assmann B, Baric I, Troncoso M, Mühlhausen C, Zschocke J, Boy NP, Hoffmann GF, Garbade SF, Kölker S (2009) Dynamic changes of striatal and extrastriatal abnormalities in glutaric aciduria type I. Brain 132:1764–1782. https://doi.org/ 10.1093/brain/awp112

[9] Strauss KA, Morton DH (2003) Type I glutaric aciduria, part 2: a model of acute striatal necrosis. Am. J. Med. Genet. C Semin. Med Genet 121C:53-70. https://doi.org/10.1002/ajmg.c.20008

[10] Zinnanti WJ, Lazovic J, Wolpert EB, Antonetti DA, Smith MB, Connor JR, Woontner M, Goodman SI, Cheng KC (2006) A diet-induced mouse model for glutaric aciduria type I. Brain 129(Pt 4):899-910. https://doi.org/10.1093/brain/awl009

[11] Mühlhausen C, Ergün S, Strauss KA, Koeller DM, Crnic L et al (2004) Vascular dysfunction as an additional pathomechanism in glutaric aciduria type I. J Inherit Metab Dis. 27(6):829-834. https://doi.org/10.1023/B:BOLI.0000045766.98718.d6

[12] Mühlhausen C, Ott N, Chalajour F, Tilki D, Freudenberg F et al. Endothelial effects of 3-hydroxyglutaric acid: implications for glutaric aciduria type I (2006) Pediatr Res. 59(2):196-202. https://doi.org/10.1203/01.pdr.0000197313.44265.cb

[13] Isasi E, Barbeito L, Olivera-Bravo S. Increased blood–brain barrier permeability and alterations in perivascular astrocytes and pericytes induced by intracisternal glutaric acid (2014) Fluids Barriers CNS 11:15. https://doi.org/10.1186/2045-8118-11-15

[14] Olivera-Bravo S, Ribeiro CA, Isasi E, Trías E, Leipnitz G et al (2015) Striatal neuronal death mediated by astrocytes from the Gcdh-/- mouse model of glutaric acidemia type I. Hum Mol Genet. 24(16):4504-4515. https://doi.org/10.1093/hmg/ddv175

[15] Olivera-Bravo S, Isasi E, Fernández A, Casanova G, Rosillo JC, Barbeito L (2016) Astrocyte dysfunction in developmental neurometabolic diseases. Adv Exp Med Biol 949:227-243. https://doi.org/10.1007/978-3-319-40764-7_11

[16] Strauss KA, Brumbaugh J, Duffy A, Wardley B, Robinson D et al (2011) Safety, efficacy and physiological actions of a lysine-free, arginine-rich formula to treat glutaryl-CoA dehydrogenase deficiency: focus on cerebral amino acid influx. Mol Genet Metab. (1-2):93-106. https://doi.org/10.1016/j.ymgme.2011.07.003

[17] Mishra A, O'Farrell FM, Reynell C, Hamilton NB, Hall CN, Attwell D (2014) Imaging pericytes and capillary diameter in brain slices and isolated retinae. Nat Protoc. 9(2):323-336. https://doi.org/10.1038/nprot.2014.019

[18] Mishra A, Reynolds JP, Chen Y, Gourine AV, Rusakov DA, Attwell D (2016) Astrocytes mediate neurovascular signaling to capillary pericytes but not to arterioles. Nat Neurosci. 19(12):1619-1627. https://doi.org/10.1038/nn.4428

[19] Hall CN, Reynell C, Gesslein B, Hamilton NB, Mishra A et al (2014) Capillary pericytes regulate cerebral blood flow in health and disease. Nature 508(7494):55-60. https://doi.org/10.1038/nature13165

[20] Cassina P, Peluffo H, Pehar M, Martinez-Palma L, Ressia A et al (2002) Peroxynitrite triggers a phenotypic transformation in spinal cord astrocytes that induces motor neuron apoptosis. J Neurosci Res. 67(1):21-29. https://doi.org/10.1002/jnr.10107

[21] Tigges U, Welser-Alves JV, Boroujerdi A, Milner R (2012) A novel and simple method for culturing pericytes from mouse brain. Microvasc Res. 84(1):74-80. https://doi.org/10.1016/j.mvr.2012.03.008

[22] Das A, Frank RN, Weber ML, Kennedy A, Reidy CA et al (1998) ATP causes retinal pericytes to contract in vitro. Exp Eye Res. 46(3):349-362. https://doi.org/10.1016/S0014-4835(88)80025-3

[23] Kawamura H, Sugiyama T, Wu DM, Kobayashi M, Yamanishi S et al (2003) ATP: a vasoactive signal in the pericyte-containing microvasculature of the rat retina. J Physiol. 551(3):787-799. https://doi.org/10.1113/jphysiol.2003.047977

[24] Attwell D, Mishra A, Hall CN, O'Farrell FM, Dalkara T (2016) What is a pericyte? J Cereb Blood Flow Metab. 36(2):451-455. https://doi.org/10.1177/0271678X15610340

[25] Giaume C, Orellana JA, Abudara V, Sáez JC (2012) Connexin-based channels in astrocytes: how to study their properties. Methods Mol Biol. 814:283-303. https://doi.org/10.1007/978-1-61779-452-0_19

[26] Armada A, Martins C, Spengler G, Molnar J, Amaral L et al (2016) Fluorimetric Methods for Analysis of Permeability, Drug Transport Kinetics, and Inhibition of the ABCB1 Membrane Transporter. Methods Mol Biol. 1395:87-103. https://doi.org/10.1007/978-1-4939-3347-1_7

[27] Olivera-Bravo S, Fernández A, Sarlabós MN, Rosillo JC, Casanova G et al (2011) Neonatal astrocyte damage is sufficient to trigger progressive striatal degeneration in a rat model of glutaric acidemia-I. PlosOne 6:e20831-20840. https://doi.org/10.1371/journal.pone.0020831

[28] Cory G. Scratch-wound assay (2011). Methods Mol Biol. 769:25-30. https://doi.org/10.1007/978-1-61779-207-6_2

[29] Aguilera KY, Brekken RA (2014) Recruitment and retention: factors that affect pericyte migration. Cell Mol Life Sci. 71(2):299-309. https://doi.org/10.1007/s00018-013-1432-z

[30] Almutairi MM, Gong C, Xu YG, Chang Y, Shi H (2016) Factors controlling permeability of the blood-brain barrier. Cell Mol Life Sci. 73(1):57-77. https://doi.org/10.1007/s00018-015-2050-8

[31] Gould IG, Tsai P, Kleinfeld D, Linninger A (2017) The capillary bed offers the largest hemodynamic resistance to the cortical blood supply. J Cereb Blood Flow Metab. 37(1):52-68. https://doi.org/10.1177/0271678X16671146

[32] Külkens S, Harting I, Sauer S, Zschocke J, Hoffmann GF et al. (2005) Late-onset neurologic disease glutaryl-CoA dehydrogenase deficiency. Neurol. 64:142-2144. https://doi.org/10.1212/01.WNL.0000167428.12417.B2

[33] Peppiatt CM, Howarth C, Mobbs P, Attwell D (2006) Bidirectional control of CNS capillary diameter by pericytes. Nature 443(7112):700-704. https://doi.org/10.1038/nature05193

[34] Hamilton NB, Attwell D, Hall CN (2010) Pericyte-mediated regulation of capillary diameter: a component of neurovascular coupling in health and disease. Front Neuroenergetics 2:5. https://doi.org/10.3389/fnene.2010.00005

[35] Olivera S, Fernandez A, Latini A, Rosillo JC, Casanova G, et al (2008) Astrocytic proliferation and mitochondrial dysfunction induced by accumulated glutaric acidemia I (GAI) metabolites: possible implications for GAI pathogenesis. Neurobiol Dis. 2008; 32: 528–34. https://doi.org/10.1016/j.nbd.2008.09.011

[36] Lindahl P, Johansson BR, Levéen P, Betsholtz C (1997) Pericyte loss and microaneurysm formation in PDGF-B-deficient mice. Science 277(5323):242-245. https://doi.org/ 10.1126/science.277.5323.242

[37] Armulik A, Abramsson A, Betsholtz C (2005) Endothelial/pericyte interactions. Circ Res. 97(6):512-523. https://doi.org/10.1161/01.RES.0000182903.16652.d7

[38] Armulik A, Genové G, Betsholtz C (2011) Pericytes: developmental, physiological, and pathological perspectives, problems, and promises. Dev Cell. 21(2):193-215. https://doi.org/10.1016/j.devcel.2011.07.001

[39] Mahfoud A, Domínguez CL, Rizzo C, Ribes (2004) In utero macrocephaly as clinical manifestation of glutaric aciduria type I. Report of a novel mutation. A Rev Neurol. 39(10):939-942. https://doi.org/ 10.1055/s-0029-1239525

[40] Davis GE, Senger DR (2008) Extracellular matrix mediates a molecular balance between vascular morphogenesis and regression. Curr Opin Hematol 15(3):197-203. https://doi.org/10.1097/MOH.0b013e3282fcc321

[41] Gerhardt H, Golding M, Fruttiger M, Ruhrberg C, Lundkvist A et al (2003) VEGF guides angiogenic sprouting utilizing endothelial tip cell filopodia. J Cell Biol. 161(6):1163-1177. https://doi.org/10.1083/jcb.200302047

[42] Argaw AT, Asp L, Zhang J, Navrazhina K, Pham T et al (2012) Astrocyte-derived VEGF-A drives blood-brain barrier disruption in CNS inflammatory disease. J Clin Invest. 122(7):2454-2468. https://doi.org/10.1172/JCI60842

[43] Chapouly C, Tadesse Argaw A, Horng S, Castro K, Zhang J et al (2015) Astrocytic TYMP and VEGFA drive blood-brain barrier opening in inflammatory central nervous system lesions. Brain 138(Pt 6):1548-1567. https://doi.org/10.1093/brain/awv077

Funding: This study was funded by the Program for the Development of Basic Sciences (PEDECIBA) a joint program of the University of the Republic (UDELAR) and the Ministry of Education and Culture (MEC). E.I. received a Doctoral Fellowship from the National Agency for Innovation and Research (ANII) and grants to attend to Prof. Attwell's lab from PEDECIBA and the Sectorial Comission for Scientific Research (CSIC, UDELAR). E.I.'s experiments in the Attwell lab were funded by a European Research Council grant to D.A. N.K. was supported by a BBSRC (UK) LIDo PhD studentship.

Conflict of interest: The authors declare that they do not have any conflict of interest

Figure captions

Fig. 1 GA induced capillary constriction in rat cortical slices. **(a)** DIC images of a longitudinal profile of a healthy capillary containing red blood cells, in basal conditions or after 20 min perfusion with aCSF containing 1 mM GA. The capillary constricts after GA exposure, near the pericyte soma. Diameters measured are shown by a red line and pericyte somata by yellow/red arrows. **(b)** Quantitation of capillary diameters measured near pericyte somata (<10 µm distance from the center of pericyte somata) and further from the soma (20-25 µm distance). Diameters were measured every 30 s in basal conditions (5 min perfusion with aCSF) and then incubated with GA (20 min perfusion of aCSF + 1mM GA). A significant reduction in capillary diameter (t-test, p<0.05, n=10) was observed after minute 12. At 25 min, there was a 16% reduction in capillary diameter compared with baseline (t-test, p=0.04). **(c)** Maximum intensity projection z-stack images of fixed cortical slices showing blood vessels with fluorescent IB4 (grey) and nuclei stained with DAPI (blue). Yellow/ red arrows are pointing pericyte somata containing nuclei and the red lines indicate the internal vessel diameters that were measured. **(d)** Graph shows the average of all vessel diameters measured < 10µm from the center of pericyte somata. There is a 23% reduction in the capillary diameter of slices exposed to GA compared with controls (*t-test, p=0.0006). A-B: living slices. C-D: fixed slices.

Fig. 2 Characterization of primary pericyte cultures from rat brain. **(a)** Images show a primary pericyte culture obtained from cortical microvessels adhered on a collagen substrate. The initial culture contained different cell types: pericytes (NG2, green), endothelial cells (von Willebrand factor, vWF, red) and astrocytes (GFAP, red). TL= transmitted light image. All panels are different fields of view. **(b)** Purified pericyte cultures, i.e. 2nd passage, on a plastic substrate, express the prototypical pericyte markers NG2 (green) and PDGFRβ (red) and appear as flattened cells with an irregular shape in close contact with one another as seen by light microscopy. All nuclei are stained with Hoechst (blue). **(c)** Response of pericyte cultures to ATP and adenosine. Upon the addition of ATP (10 µM, 1 hr), cultured pericytes adopted a stellate shape with somata becoming rounded and smaller and cellular processes emerging as shown by ethidium bromide staining (EtBr, red). In contrast, pericytes exposed to adenosine (Ado, 10 µM, 1 hr) maintained a flattened morphology, similar to controls. TL: Transmitted light microscopy.

Fig. 3 Absence of GA effect on contraction of cultured isolated pericytes. **(a)** DIC images merged with Hoechst fluorescence show pericytes incubated in a cell culture chamber with 5 mM GA, 100 µM ATP (positive control) or vehicle (control) for 2 hr. Only ATP exposure caused visible morphological changes that appear as a reduction of soma and nuclei size with emergence of conspicuous cellular processes. Arrowheads show individual cells in all conditions mentioned above. **(b)** Confocal images show phalloidin (Phall) staining (red) and Hoechst stained nuclei in pericyte cultures. A visible actin cytoskeleton re-arrangement is seen in the ATP condition compared with controls, with pericyte processes becoming more clearly visible. Arrowheads point at individual cells. Below, images at higher magnification are shown. **(c)** Graph shows the percentage of contracted cells (relative to total cells). This value is significantly increased in the ATP condition, but not in GA-treated cells, compared with controls. Kruskal-Wallis test and Dunn's multiple comparison ***p=0.0004; **p=0.003 were employed. N.S: statistically not significantly different. **(d)** Living pericyte cultures were imaged every 1 min in basal condition and after the addition of 5 mM GA, 100 µM ATP or vehicle (controls) for 35 min. **(e)** Graph shows the quantitation of cell-free area, normalized with respect to time 0, every 5 min for the three experimental conditions: control, GA and ATP-treated cells. With ATP added to the medium, there is a significant increase in cell-free area from minute 25 to 35 with respect to controls, indicating cell contraction. Two-way ANOVA and Dunn's multiple comparisons *p=0.02; **p=0.006; **' p=0.002.

Fig. 4 Astrocyte conditioned media induces pericyte contractility in cell cultures. **(a)** Light microscope images of pericyte cultures in control conditions and when incubated with conditioned media from control astrocytes (CM-C) or GA-treated astrocytes (CM-GA) for 2 hr. A conspicuous morphological change is observed with CM-C and CM-GA that resembles ATP-induced contraction and includes a reduction of soma and nuclei size and the appearance of more visible cellular processes. Individual pericytes are indicated with white arrows. **(b)** Graph shows a significant increase in the percentage of contracted cells defined as cells with a conspicuous morphological change described as above. Kruskal-Wallis test and Dunn's multiple comparison correction, ***' p=0.0002, **** p<0.0001.

Fig. 5 Conditioned medium from GA-treated astrocytes inhibits pericyte migration and delays scratch closure in cultures. **(a)** Light microscopy images show pericytes in a scratch wound assay at 0,

24 and 48 hr incubated with 5mM GA, or with conditioned medium from control (CM-C) or from GA-treated (CM-GA) astrocytes. Although there is a reduction in cell-free area in all experimental conditions over time due to pericyte proliferation and migration, CM-GA exposure caused a delay in the closure of the scratch as shown by a larger cell-free area. The last column shows fluorescent images of Hoechst-stained nuclei (blue) and mitotic cells (BrdU+, green) at 48 h in the scratch region in all experimental conditions. Black and white dashed lines encircle cell-free areas. **(b)** Quantitation of cell-free area at 24 and 48 hr, as a percentage of that at 0 hr, shows significantly larger cell-free areas in the CM-GA condition with respect to controls. Kruskal-Wallis test and Dunn's multiple comparison, * p=0.01, **p=0.005. **(c)** Graph shows the number of nuclei stained with Hoechst in the scratch area at 48 hr. Quantitation confirmed that CM-GA caused a larger reduction in the cell number of the scratched area when compared to CM-C. One-way ANOVA and Tukey's multiple comparison, ** p=0.002; **'p=0.008. **(d)** Graph shows the rate of proliferating cells defined as %BrdU+ cells/ Hoechst+ cells in the scratched area at 48h. There were no differences in the proliferation rate which was between 52 and 58% in all experimental groups.

Fig. 6 Secretome analysis of astrocyte CM-C and CM-GA. Cytokine levels in concentrated aliquots of CM-C and CM-GA containing the same amount of total protein were assessed with a commercial array according to manufacturer instructions. **(a)** Two representative images that show the expression of 34 soluble cytokines in membranes exposed to CM-C or CM-GA and detected by chemiluminiscence with a CCD camera. Spots inside the red rectangle are positive controls and inside the blue rectangle are the negative controls. Each spot corresponds to the expression of a cytokine. Each cytokine is represented by 2 measurements in one membrane**. (b)** The graph represents the normalized spot signal (mean ± SEM) for each cytokine analyzed in CM-C and CM-GA obtained in simultaneous experiments. **(c)** The graph shows the n-fold increase between normalized cytokine signals in CM-GA vs CM-C.

Supplementary Fig. 1 GA does not affect pericyte survival in brain slices or in primary culture. (a) Maximum intensity projection z-stack images showing a capillary in a control or GA-treated slice stained with fluorescent IB4 (green, to label capillary walls) and nuclei with DAPI (blue). **(b)** Graph shows the absence of differences in the number of dead (propidium iodide (PI) positive) pericytes expressed as a percentage of total cells, that were found in a 10 µm deep stack in control and GA (1 and 5 mM) treated slices. **(c)** Pericyte primary cultures from rat brain were immunostained to detect PDGFRβ (top panel) or incubated with fluorescent phalloidin to visualize actin filaments (lower panel). After 24 hr exposure to GA, there are no significant morphological changes in actin cytoskeleton or PDGFRβ expression. **(d)** Graph shows no difference in cell viability by using a sulforhodamine B assay in cultures treated with 1 and 5 mM GA (24 h) compared with controls. **(e)** Quantitation of PDGFRβ fluorescence by measuring the mean gray value (MGV) in pericyte cultures shows no difference between GA-treated (5mM) cells and controls. N.S: statistically not significantly different.

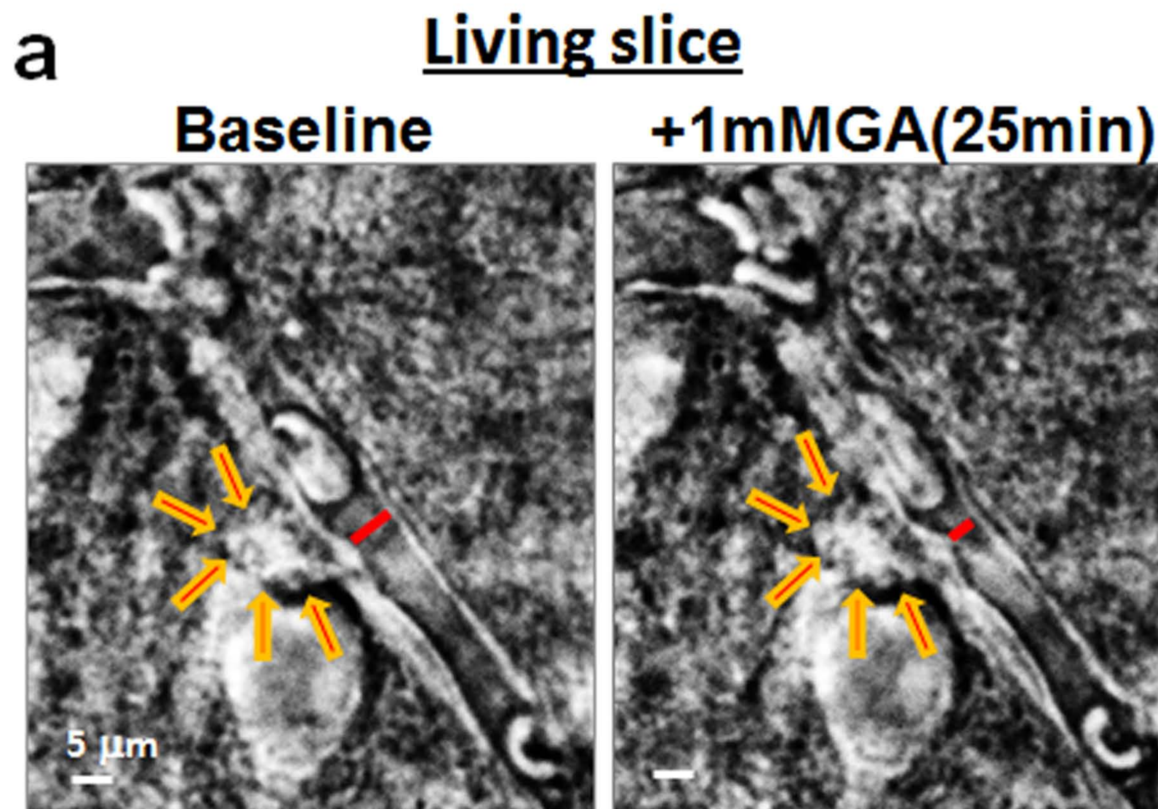
a
Living slice
Baseline
+1mMGA(25min)
5 µm

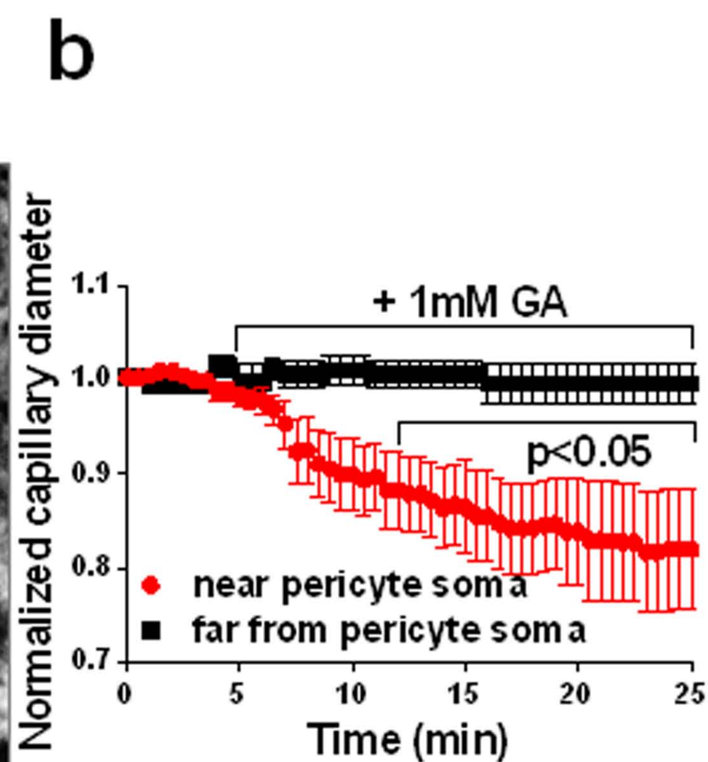
b
Normalized capillary diameter
+ 1mM GA
p<0.05
near pericyte soma
far from pericyte soma
Time (min)
1.1
1.0
0.9
0.8
0.7
0
5
10
15
20
25

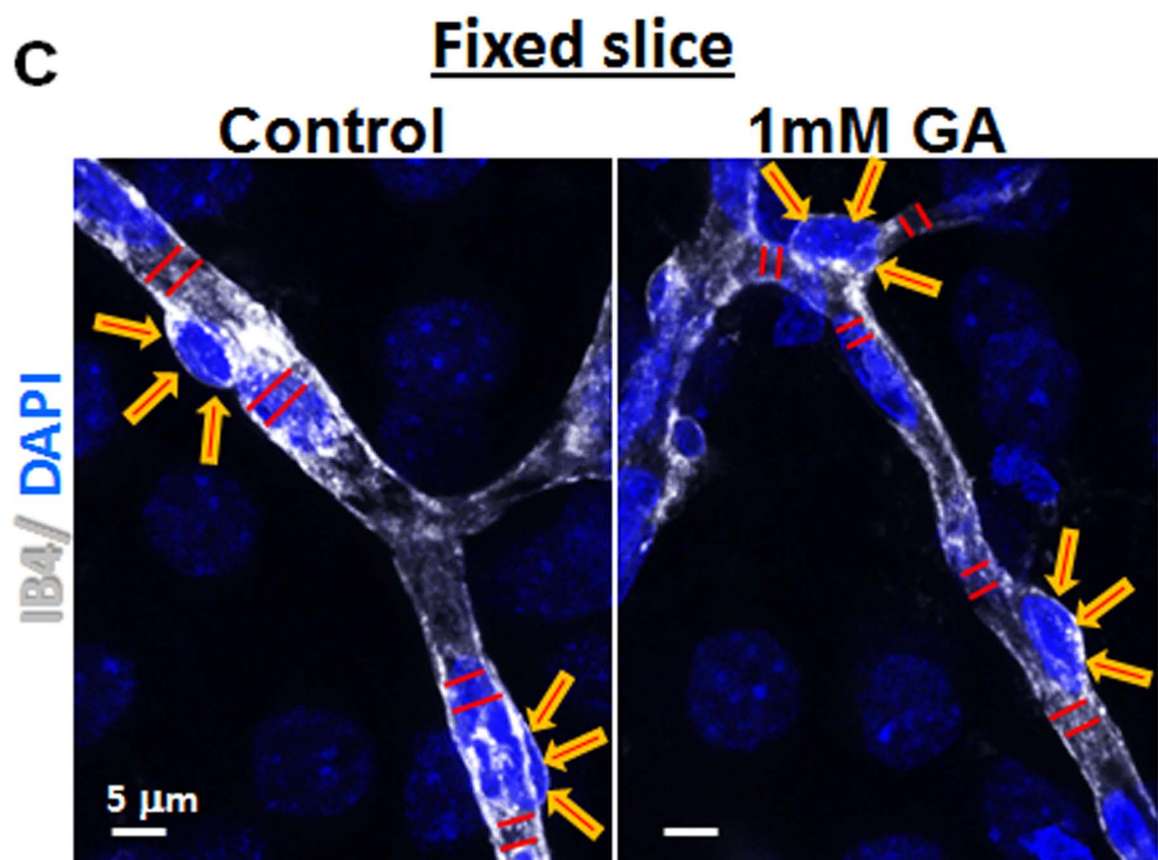
c
Fixed slice
Control
1mM GA
IB4/ DAPI
5 µm

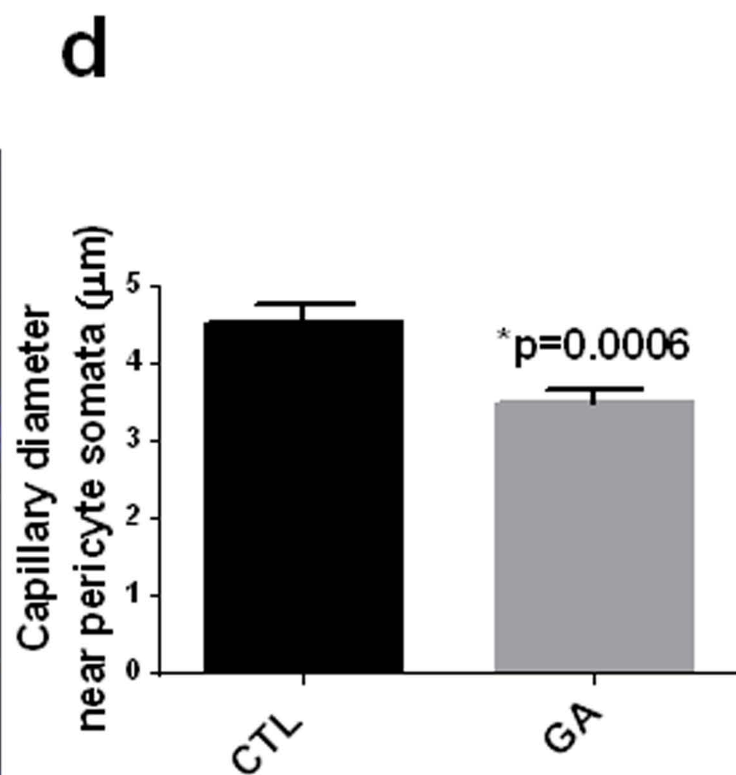
d
Capillary diameter near pericyte somata (µm)
*p=0.0006
0
1
2
3
4
5
CTL
GA

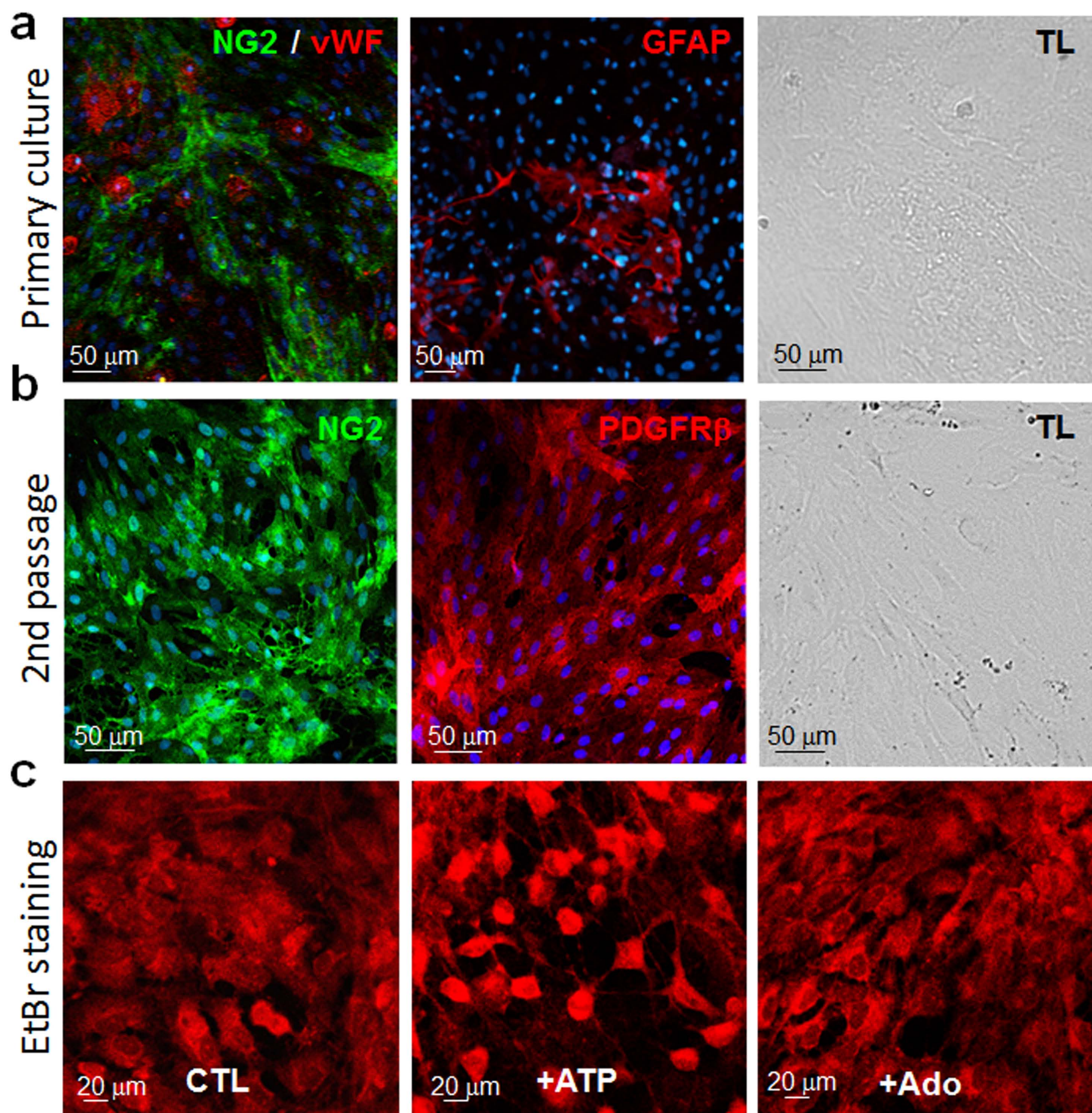
a
NG2 / vWF
GFAP
TL
Primary culture
50 µm
50 µm
50 µm
b
NG2
PDGFRβ
TL
2nd passage
50 µm
50 µm
50 µm
c
EtBr staining
20 µm
CTL
20 µm
+ATP
20 µm
+Ado

a

CONTROL

5mM GA

100μM ATP

DIC/ Hoechst

50 μm

b

Phall / Hoechst

50 μm

25 μm

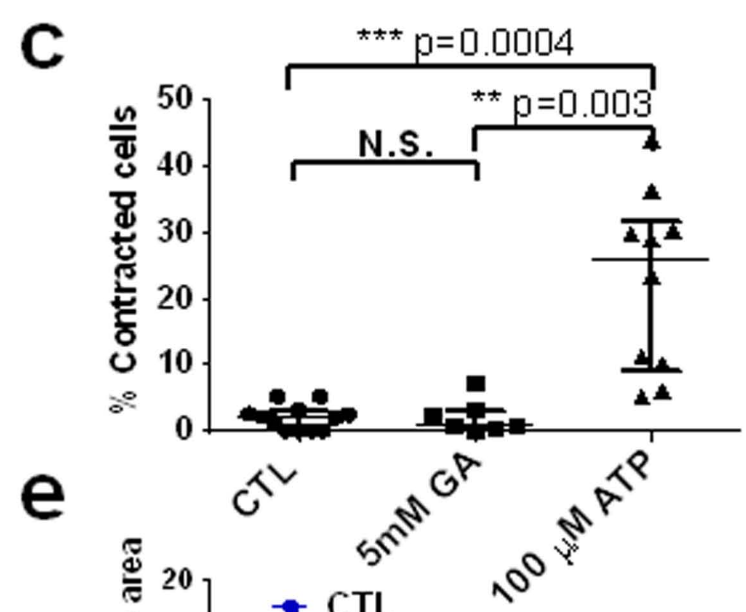

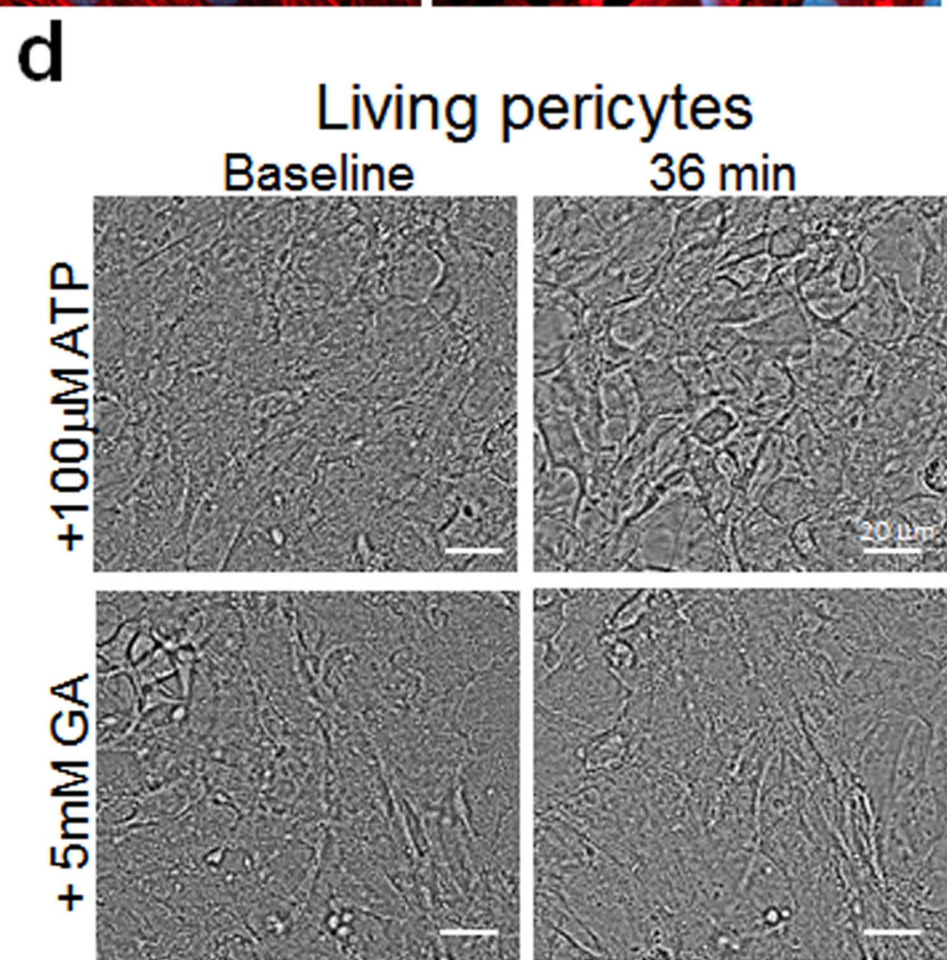

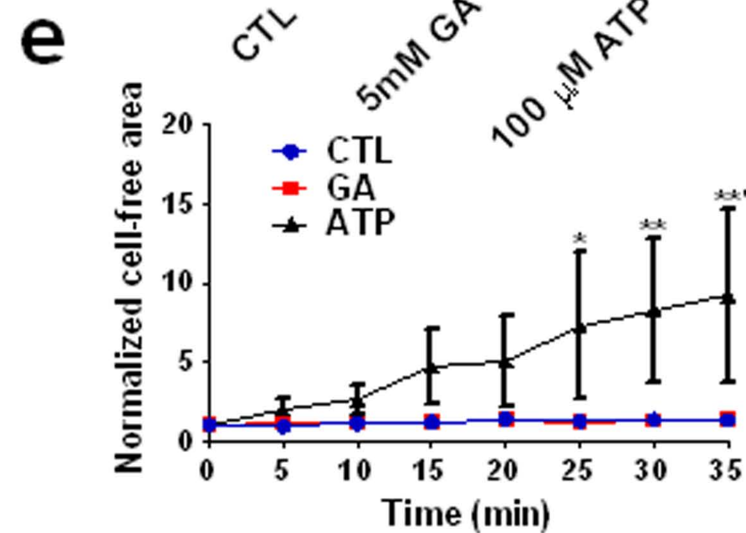

a

CONTROL CM-C CM-GA

20 µm

b

N.S.

***p=0.0002

****p<0.0001

% Contracted cells

0 10 20 30 40 50

CTL CM-C CM-GA

a

t=0 h
t=24 h
t=48 h
BrdU/ Hoechst
CONTROL
5mM GA
CM-C
CM-GA
100 µm
50 µm

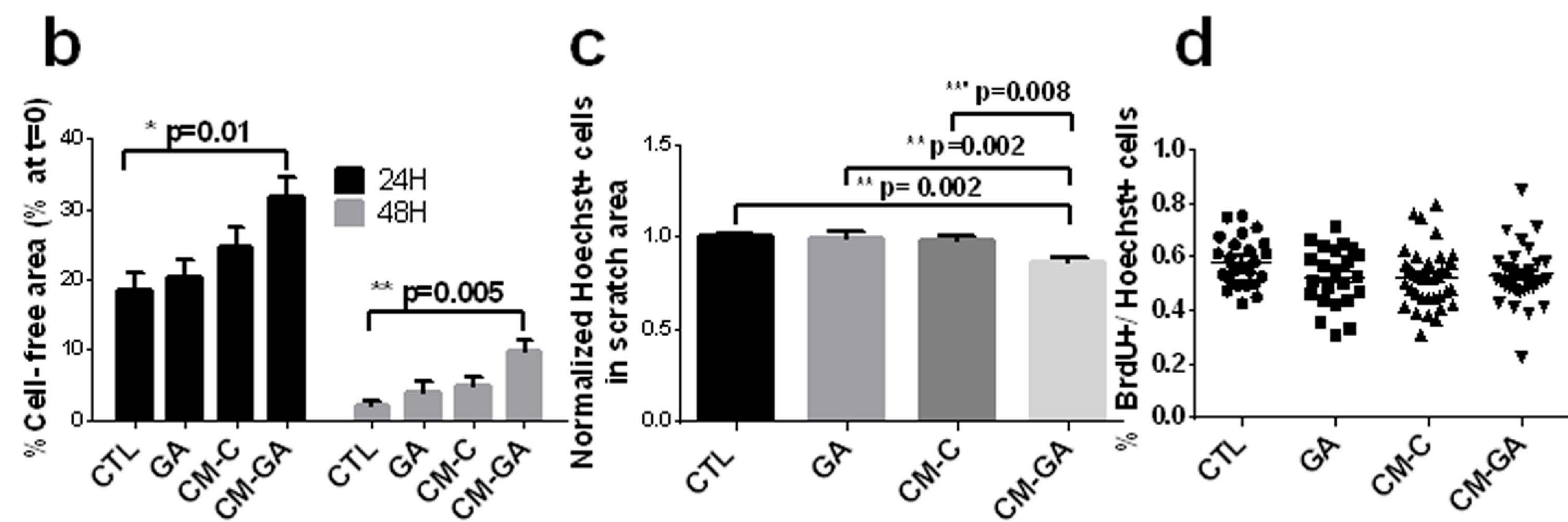

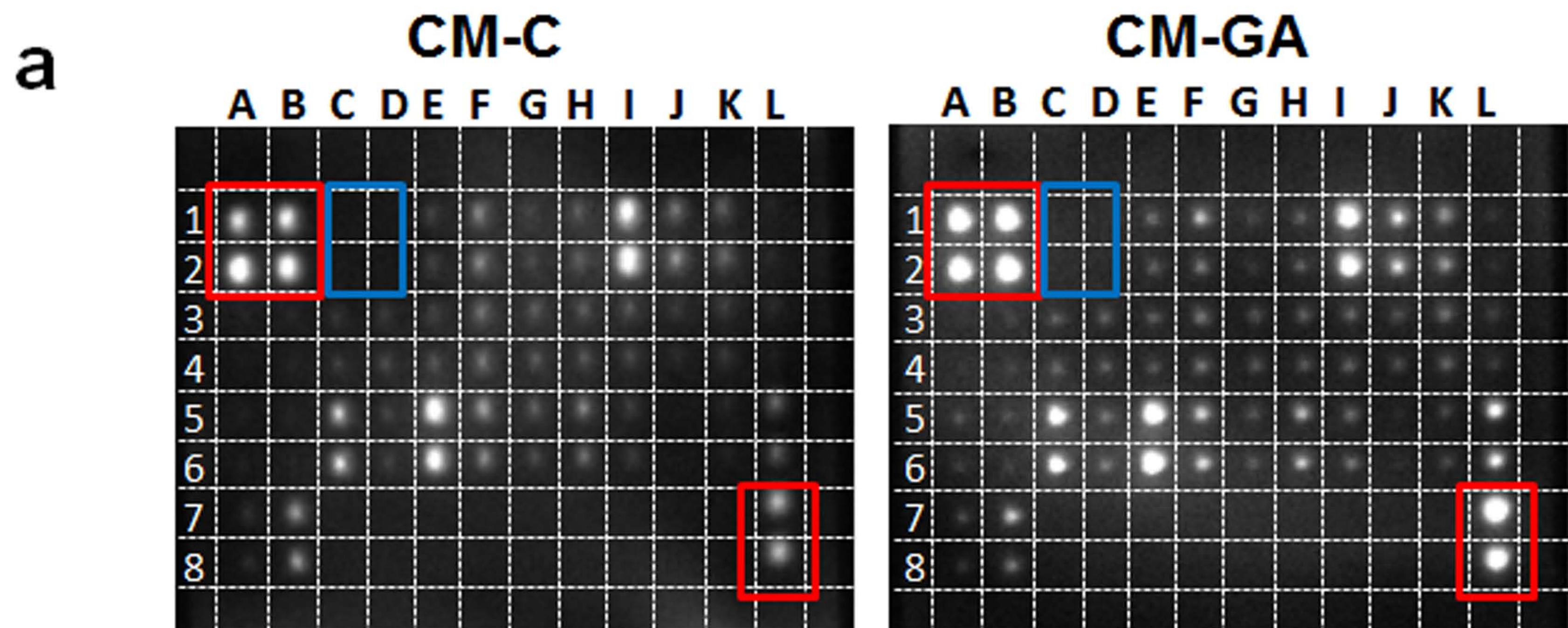
a
CM-C
CM-GA
A B C D E F G H I J K L
1
2
3
4
5
6
7
8

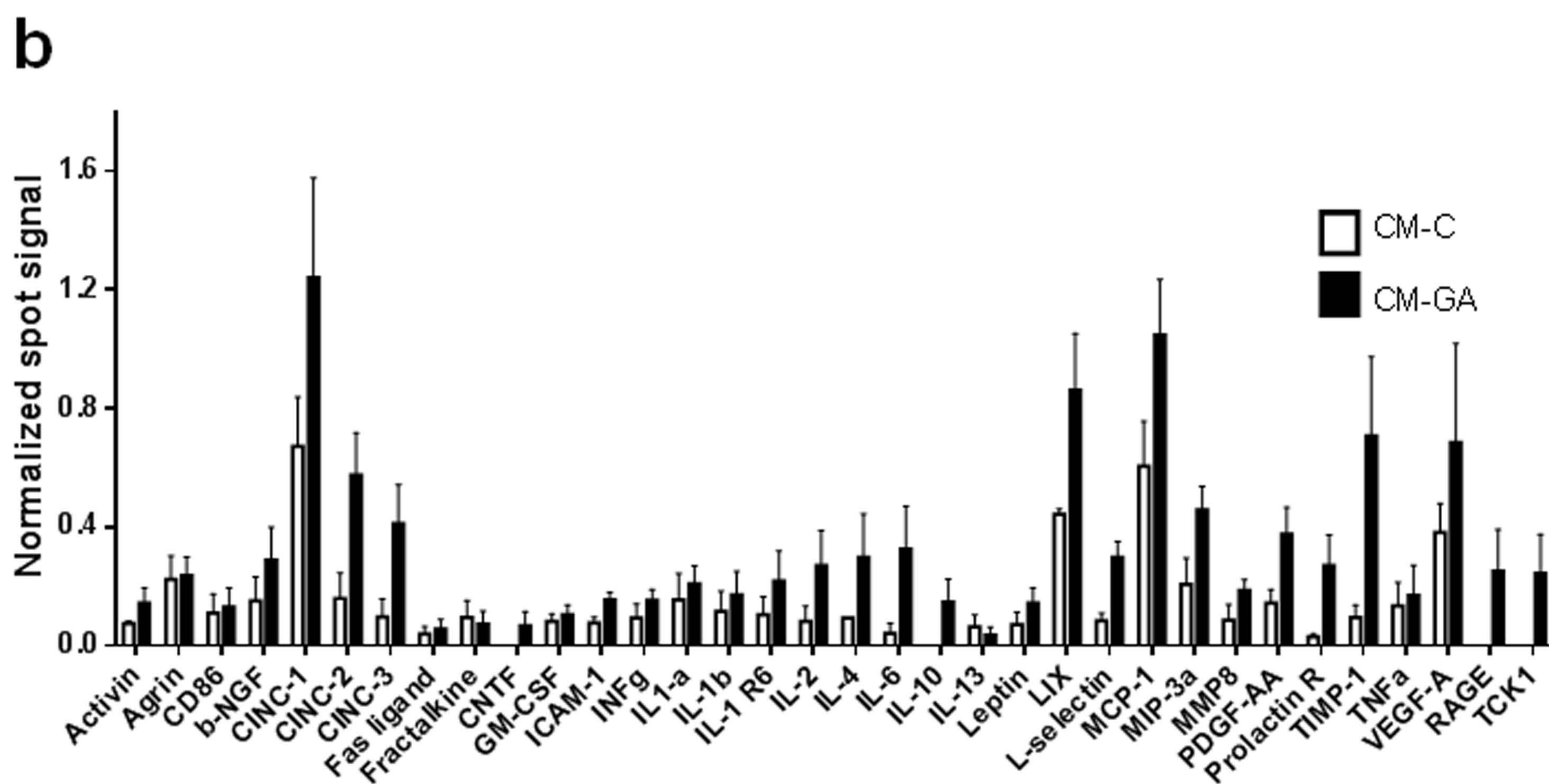
b
Normalized spot signal
1.6
1.2
0.8
0.4
0.0
CM-C
CM-GA
Activin
Agrin
CD86
b-NGF
CINC-1
CINC-2
CINC-3
Fas ligand
Fractalkine
CNTF
GM-CSF
ICAM-1
INFg
IL1-a
IL-1b
IL-1 R6
IL-2
IL-4
IL-6
IL-10
IL-13
Leptin
LIX
L-selectin
MCP-1
MIP-3a
MMP8
PDGF-AA
Prolactin R
TIMP-1
TNFa
VEGF-A
RAGE
TCK1

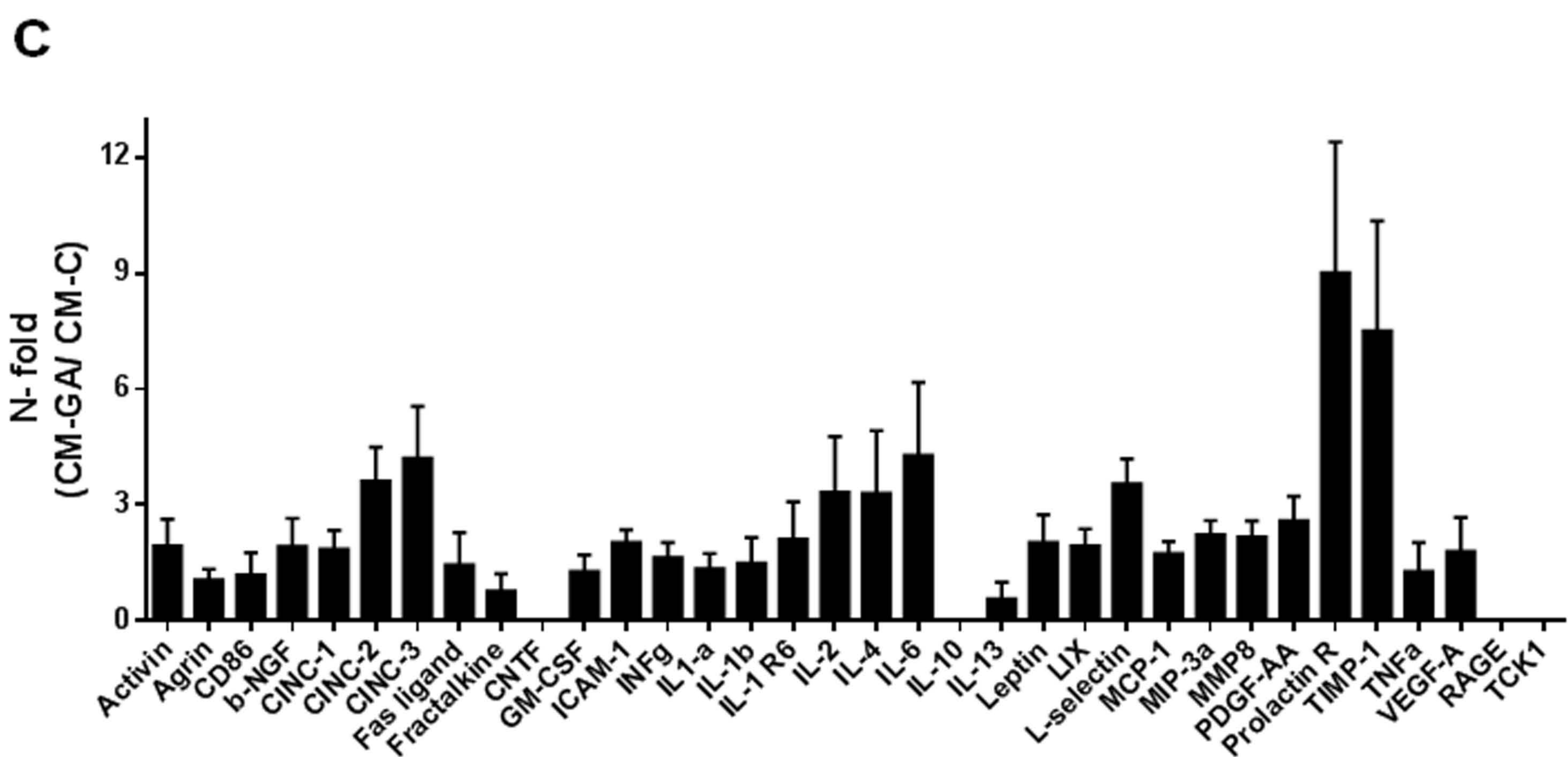
c
N- fold
(CM-GA/ CM-C)
12
9
6
3
0
Activin
Agrin
CD86
b-NGF
CINC-1
CINC-2
CINC-3
Fas ligand
Fractalkine
CNTF
GM-CSF
ICAM-1
INFg
IL1-a
IL-1b
IL-1 R6
IL-2
IL-4
IL-6
IL-10
IL-13
Leptin
LIX
L-selectin
MCP-1
MIP-3a
MMP8
PDGF-AA
Prolactin R
TIMP-1
TNFa
VEGF-A
RAGE
TCK1

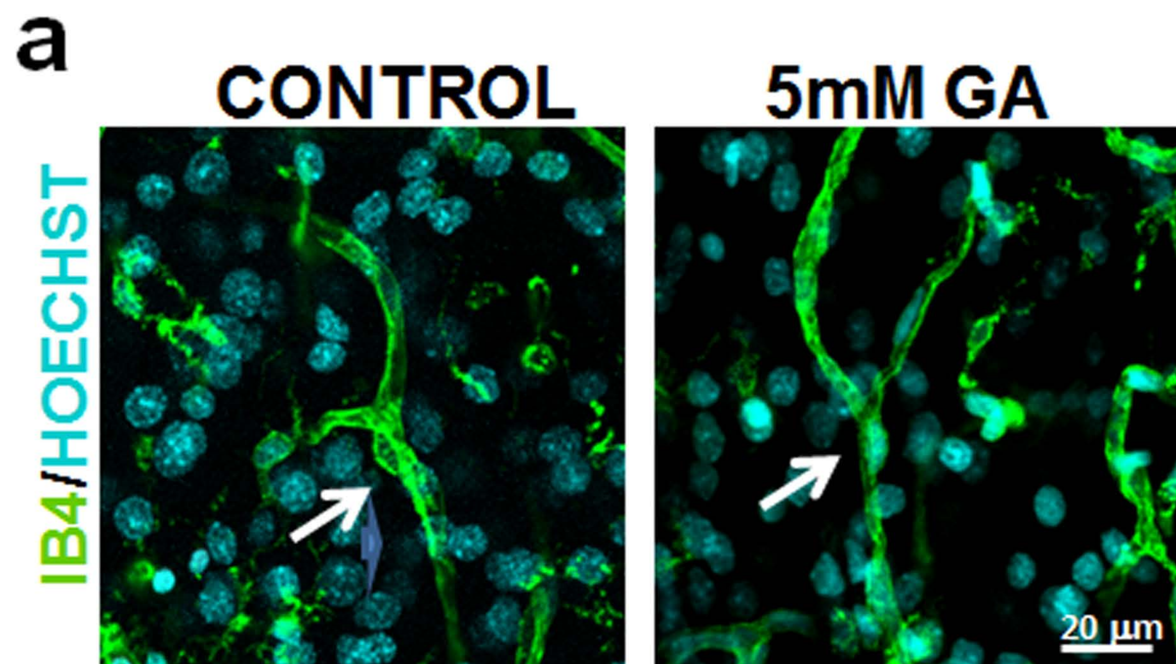
a
CONTROL
5mM GA
IB4/HOECHST
20 µm

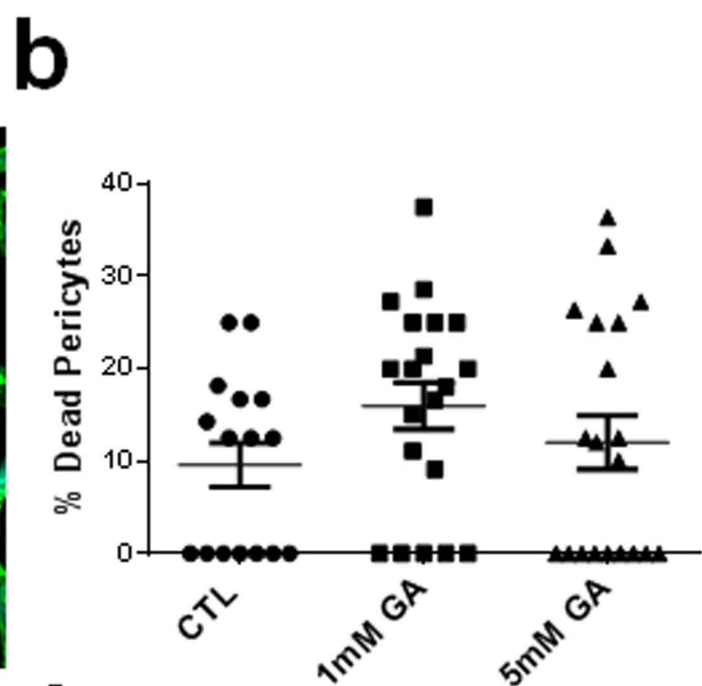
b
% Dead Pericytes
40
30
20
10
0
CTL
1mM GA
5mM GA

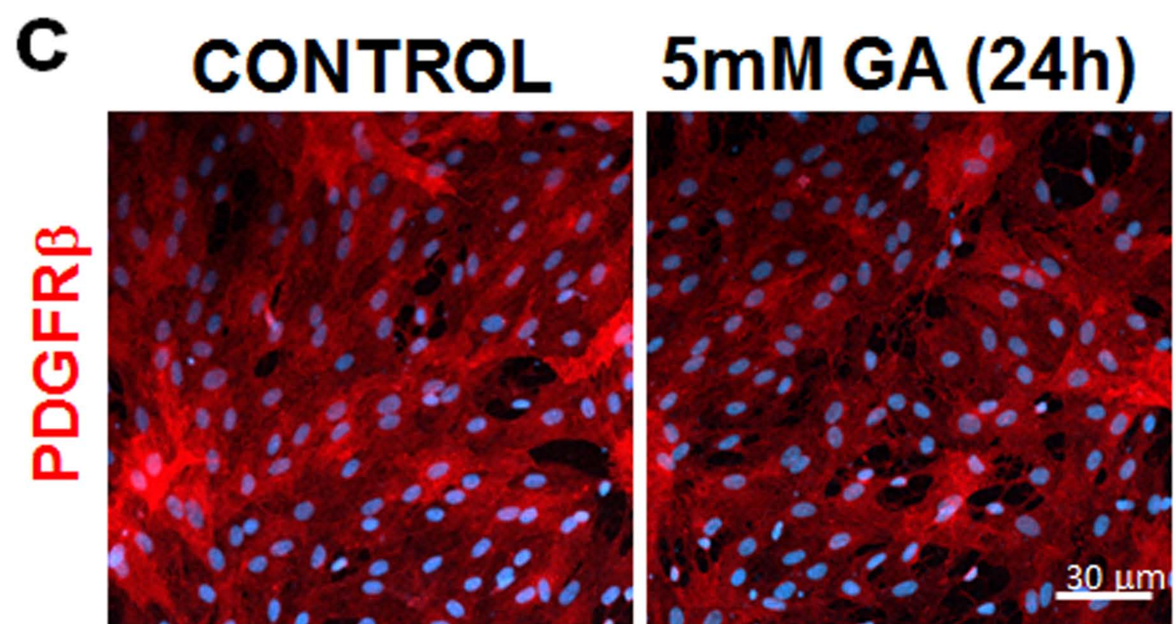
c
CONTROL
5mM GA (24h)
PDGFRβ
30 µm

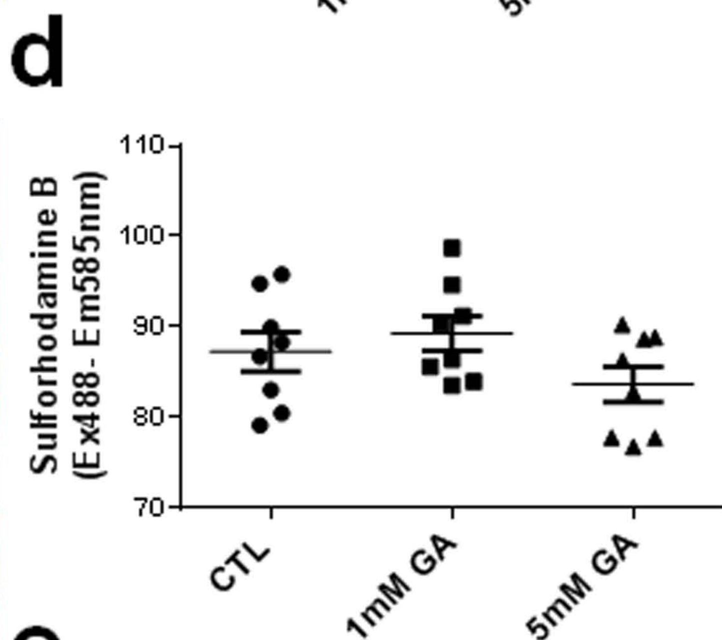
d
Sulforhodamine B
(Ex488- Em585nm)
110
100
90
80
70
CTL
1mM GA
5mM GA

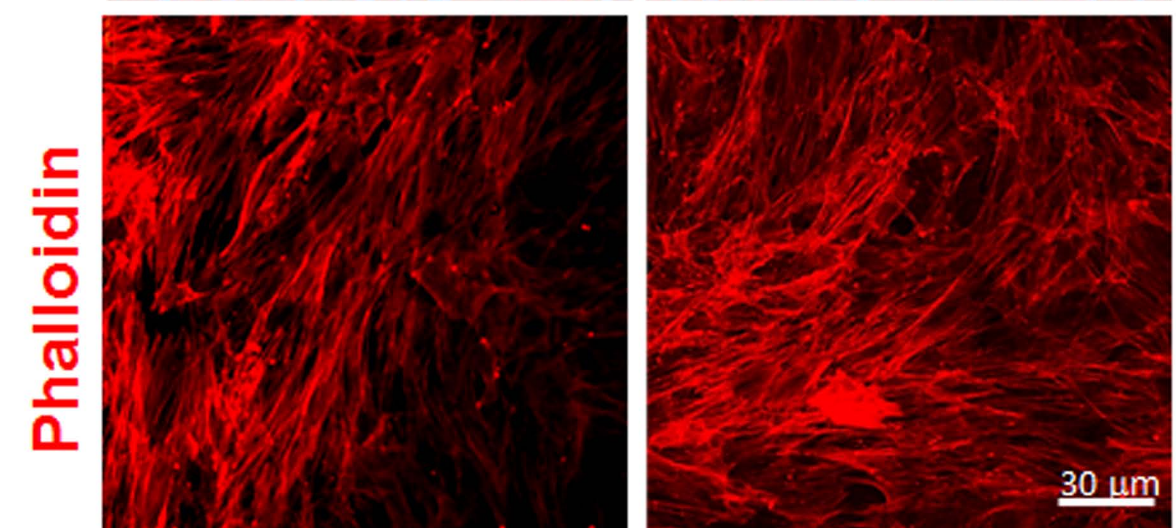
Phalloidin
30 µm

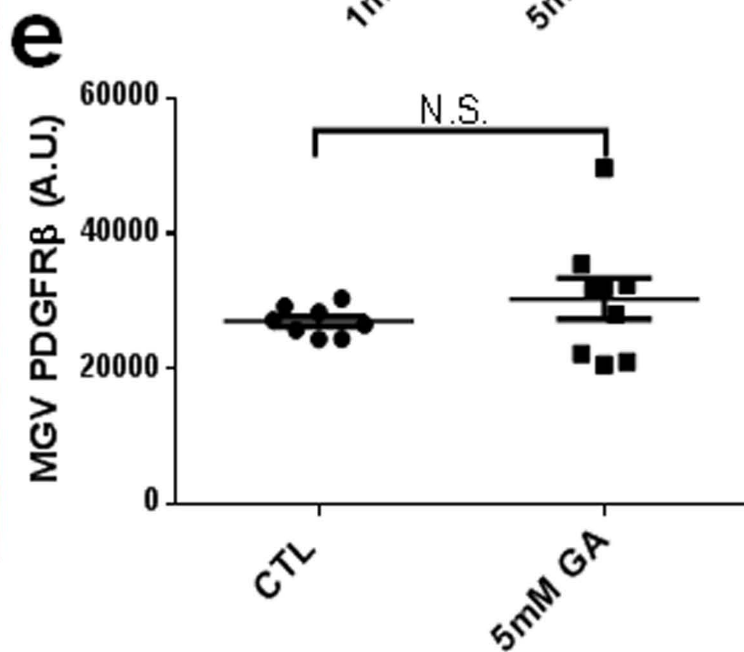
e
MGV PDGFRβ (A.U.)
60000
40000
20000
0
N.S.
CTL
5mM GA